''Hollow cathode'' gun optics

G. Ciullo
INFN Laboratori Nazionali di Legnaro, I-35020 Legnaro, Italy and CNR-Centro di Fisica degli Stati Aggregati, I-38050 Povo, Italy

A. N. Sharapa and A. V. Shemyakin
Institute of Nuclear Physics, 630090 Novosibirsk, Russia

L. Tecchio
Dipartimento di Fisica Sperimentale dell'Università and INFN, 1-10125 Torino, Italy

(Received 29 May 1996; accepted for publication 22 November 1996)

The generation of an electron beam by a hollow cathode gun in a cusp magnetic field is discussed. Such a gun is proposed for an electron cooling device without toroids. In a section with a homogeneous magnetic field, this beam experiences a disturbance region near the axis where the electron temperature becomes higher. The main purpose of the article is to define conditions for generating the beam so as to restrict the extent of this region as much as possible. It is shown that a state with a virtual cathode in the vicinity of the zero magnetic field point is the most suitable for this aim. The experimental and essential analytical results are presented. © *1997 American Institute of Physics.* [S0034-6748(97)01803-0]

I. INTRODUCTION

The electron cooling device is a well-known and tested technique for cooling ions in storage rings.[1] The efficiency of the method is strictly related to the electron beam parameters.

Standard electron devices in storage rings make use of bending magnets to guide the electron beam into the cooling region. At both ends of the cooling section, the ions are slightly deflected by the transverse component of the toroidal magnetic fields which disturb the beams. These perturbations limit cooler performance. This problem can be solved by adopting an electron cooling device with no bending magnet, thus avoiding perturbations in the electron and ion beams and also enhancing cooling efficiency. A scheme for an electron cooling device without toroids was proposed in Ref. 2. The preliminary results of experiments with a prototype of such a device, developed within the framework of the CRYSTAL storage ring project,[3] are described in Ref. 4. This article continues with an investigation of the most delicate part of such a device, i.e., the ''hollow cathode'' gun.

II. GENERAL CONSIDERATIONS

A basis for selecting the electrode geometry for the hollow cathode is deduced from an analytical solution for electrostatic transformation of a disk-shaped beam into a cylindrical one (Fig. 1), the scheme of the gun that was tested is shown in Fig. 2, as described in Ref. 5. A peculiarity of this solution is zero potential values and an electric field strength in the point O in Fig. 1:

$$U_0=0, \quad E_0=0 (r=0,\ z=0). \tag{1}$$

The region near the point O is like a virtual cathode, with the corresponding potential distribution (solid curves in Fig. 3). In fact, this state can only be achieved for a strictly determined current:

$$I_0=P_0\cdot U_a^{3/2}. \tag{2}$$

This current is the full analog of a space-charge limited current in an ordinary Pierce-type electron gun. The value of P_0 can be considered as the perveance in the region where the beam is generating. In the ideal solution, all trajectories and all equipotentials are similar. This means that the full current flowing inside the equipotential U is proportional to the $U^{3/2}$, i.e., the value of P_0 does not depend on the choice of the equipotential: it can be calculated and is equal to 78 μP.

It is useful to analyze two different parts of the gun separately, i.e., a region near the cathode (I in Fig. 1) and a region where the ''cylindrical'' beam is ''generating'' II. Using such an approach, the current emitted by the cathode in a space-charge limited conditions is determined only by the anode potential U_0 and by the electrode geometry of the region I, i.e., by a geometrical perveance P_g:

$$I=P_g U_a^{3/2}, \qquad P_g=\frac{2.3\cdot S}{D_g^2}\,\mu P, \tag{3}$$

where S is a cylindrical cathode surface and D_g is an effective gap between the anode and the cathode.[6]

For a fixed ratio of gun electrode potentials, the maximum possible current I_0 passing through the region II is proportional to $U_a^{3/2}$. Therefore, the perveance P_0 (2) can be introduced in this region for the real gun.

The ideal solution assumes the presence of the zero potential surface, properly represented by a cone-shaped electrode, so cone and beam axes coincide. But the gun under consideration is designed for an electron cooling device without toroids, where the cooled beam of heavy particles travels along the axis. Actually, instead of a cone, a tube-shaped electrode (gun reflector) with potential near the cathode one is used to lower the potential in the point O.

In this case, state (I) (i.e., the state with $E_0=0$, $U_0=0$) is unstable and does not happen. This is a well-known effect for systems with space-charge limited currents. The simplest

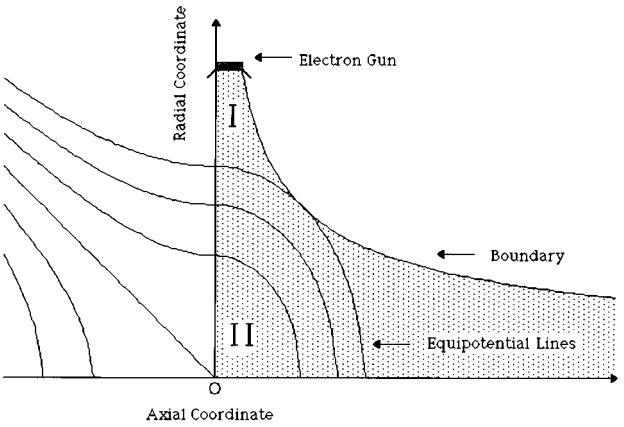

FIG. 1. An analytical solution for an electrostatic transformation of a disk-shaped beam into a cylindrical one.

example of such a system is the flat flow of electrons between two plates with potentials U_a. If there is no reflection of electrons, the minimum possible value $U_{\min}$ of the potential between plates is[6]

$$U_{\min}=0.25\cdot U_a \tag{4}$$

and it is reached only for the maximum possible current. Similar limitations for a minimum potential value also appear in devices with an intense electron beam energy recovery.[7] The instability of state (I) means that in a real gun, for the limit current I_0, another state occurs in the region II [curve 3 in Figs. 3(a) and 3(b)]:

$$U_0=U_{\min},\quad E_0=E_{\min}(z=0,\ r=0). \tag{5}$$

The closer the values $U_{\min}$, $E_{\min}$ are to zero, the closer the transformation comes to the ideal one. Our criterion for choosing the geometry of gun electrodes and their potentials was the minimization of the values of $U_{\min}$ and $E_{\min}$ for a fixed current. The behavior of potential and electric field distributions in the vicinity of the point O [Figs. 3(c) and 3(d)] is similar to the one in a planar diode (i.e., in the one-dimensional flow between two plates with potentials 0 and U_a, which is the basis for the Pierce gun). This analogy

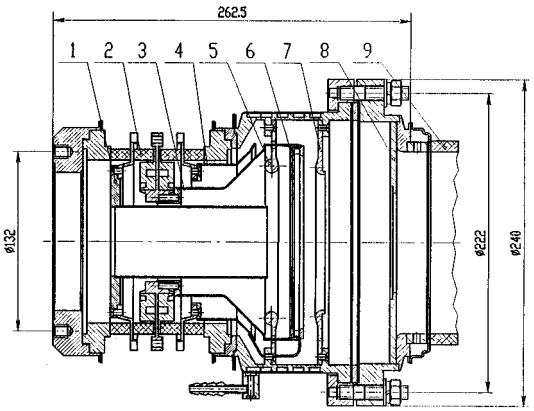

FIG. 2. Drawing of the hollow cathode gun. (1) Reflector, (2) insulator, (3) cathode feedthrough, (4) cathode heater feedthrough, (5), (7), and (8) anodes, (6) cathode, and (9) high-voltage insulator.

is emphasized by the presence of a guiding magnetic field preventing disturbed electrons from reaching the electrodes.

Three different cases can be distinguished, depending on the current density emitted by the cathode surface J_{cath} (saturation current) and the space-charge limited current density of the diode J_0.

In saturation conditions ($J_{\text{cath}}<J_0$), all emitted electrons reach the anode plate. In this case, a nonzero electric field appears near the cathode surface. In the corresponding case for the transformation zone, when $P_0>P_g$, the electric field strength and potential near the point O increase (curve 2 in Fig. 3):

$$E_0>E_{\min},\quad U_0>U_{\min}. \tag{6}$$

When the saturation current limit is reached ($J_{\text{cath}}=J_0$), the electric field near the cathode goes to zero. Such a case corresponds to the situation with $P_0=P_g$. The values of E_0, U_0 reach their minimum.

In space-charge limited conditions ($J_{\text{cath}}>J_0$), a virtual cathode is created near the real one. Electrons are reflected by this virtual cathode and the diode current remains equal to the space-charge limit.

In a case with $P_0<P_g$, such an equilibrium is also reached by means of electrons reflected by the virtual cathode appearing near the point O. They travel along magnetic field lines between the real and virtual cathodes, their additional space charge decreases in potential near the cathode, and the current going to the region II decreases. The state with reflected electrons cannot be analyzed practically by computer simulations and is investigated experimentally, therefore comparisons between experiments and simulations are possible only in saturation conditions $P_0>P_g$.

It is worth noting that, in the ideal solution (Fig. 1), the space charge is of crucial importance. It is evident that, for the fixed anode potential and a zero current, we have

$$E_0=\infty(r=0,z=0) \tag{7}$$

and particle trajectories are drastically disturbed. Generally, we do not have solution for an effective transformation without using space charge effects. Reference 5 showed that the ideal solution can be combined with the magnetic field of the cusp (a field created by two oppositely polarized solenoids), because the ideal solution trajectories coincide with the magnetic field lines of the cusp in the vicinity of the point O. Far enough from this region, the magnetic field strength is high. Here electrons are frozen and move along field lines adiabatically, and it is not necessary to match the ideal solution trajectories and field lines strictly. But the magnetic field strength is zero in the point O, and condition (1) is mandatory to obtain an electron beam without perturbations.

In a real gun with nonzero values, E_0, U_0 [Eq. (5)], the transverse motion of electrons is excited near the beam axis and, as a result, a region with higher transverse electron energies appears (disturbance region). The diameter D_d of this disturbance region can be defined with a fair degree of accuracy because, as a rule, the value of a transverse energy δW decreases exponentially with the trajectory radius [Fig. 4(a)]. In experiments, the boundary of this region is determined by the precision of δW measurements, which is 0.1 eV. The

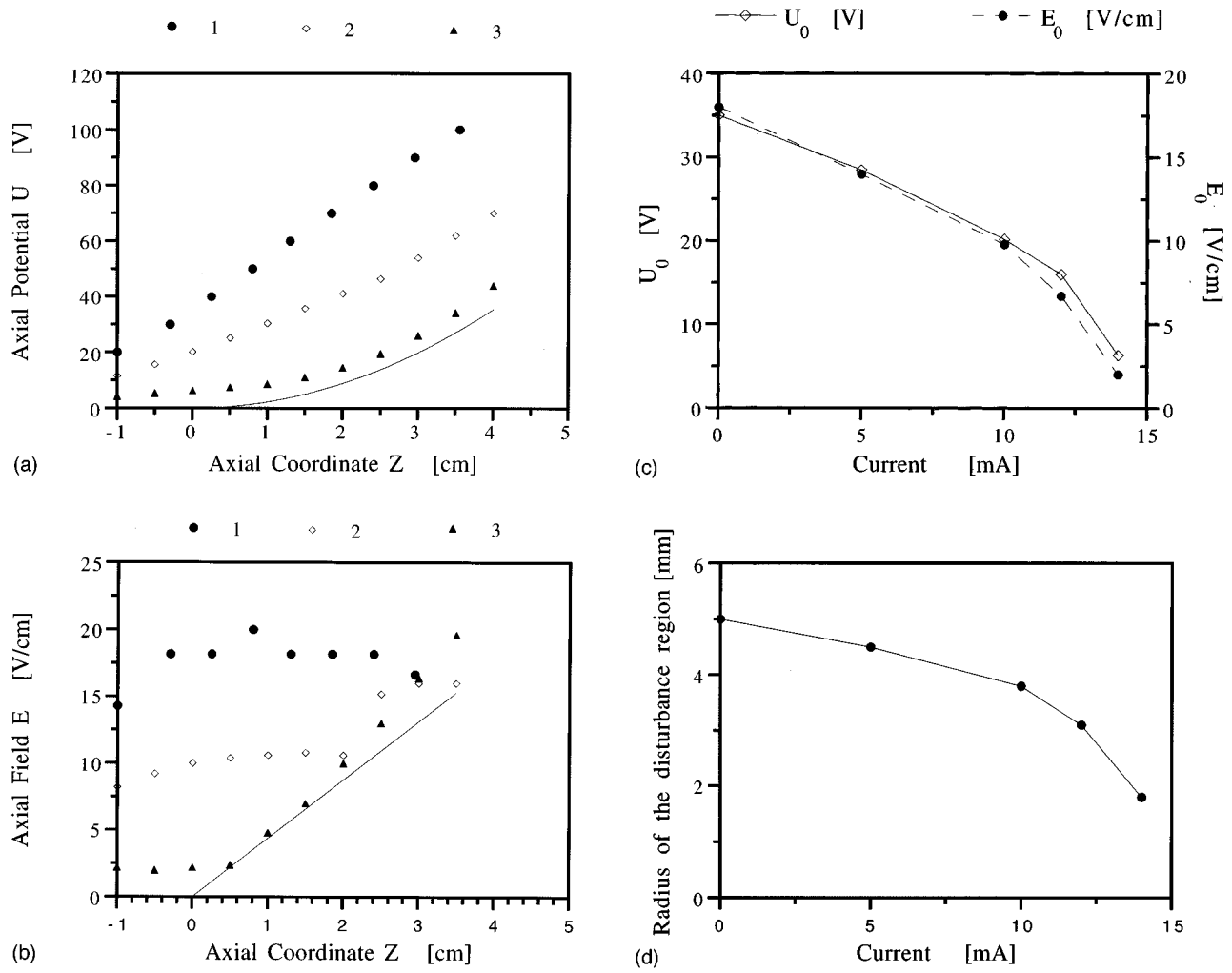

FIG. 3. Potential and electric field in the vicinity of the point O. All electrode potentials are kept at fixed values. (a) and (b) Distributions along the Z axis of potential and electric field strength, respectively, for different currents; (c) and (d) values of U_0, E_0 and the radius of disturbance region as functions of the current emitted into region II. Solid line illustrates distributions in the ideal solution. Signs show results of simulation for the real gun: (1) $I=0$ mA, (2) $I=10$ mA ($P_g<P_0$), (3) $I=14$ mA ($P_g=P_0$).

diameter D_d increases with E_0, U_0 and its size is one of the main criteria defining beam quality. The value of D_d increases with U_a and a decrease in the magnetic field strength B_0. This is illustrated in Fig. 4(b), showing the results of low perveance ($P_g=3.8$ μP) gun simulations forming part of the SuperSAM program.[8]

III. EXPERIMENTAL RESULTS

The experimental investigation was made using the setup described in Ref. 4. Table I shows some of the device parameters. Measurements were taken by means of a longitudinal energy analyzer,[9] which allows for the measurement of the longitudinal energy of electrons in a small part of the beam cut by a hole with a diameter of 0.2 mm. If the electron motion is disturbed in the gun, a transverse rotation is excited and the longitudinal energy shifted to the value δW equal to the transverse energy. Several gun geometries were tested. Differences between them were primarily in the value of the perveance P_g. One of the geometries is shown in Fig. 2. The value of P_g for this gun is 15 μP. One of the experimental goals was to achieve the state with an emitted current equal to the limit current I_0 in the region II. In measurements for the gun geometry, shown in Fig. 2, we found $P_g>P_0$.

By decreasing the cathode heater power, we can decrease the cathode emission, and consequently also the effective value of P_g. As a result, we can observe cases of different P_g and P_0 ratios. The experimental dependence $D_d=\int(P_g)$ definitely has nonmonolonous behavior (Fig. 5, curve 5). For low values of P_g, the disturbance region diameter decrease with respect to P_g, but if the current emitted

TABLE I. Parameters of the experimental device.

Magnetic field strength in drift region	1–2 kG
Electron energy in drift tube	0.1–20 kV
Beam current	1 mA–1 A
Distance between gun and analyzer	85 cm
Vacuum	3×10^{-8}–10^{-5} Pa
Cathode	
Emitter	BaO
Diameter	130 mm
Width	4 mm
Beam diameter in drift region	30 mm

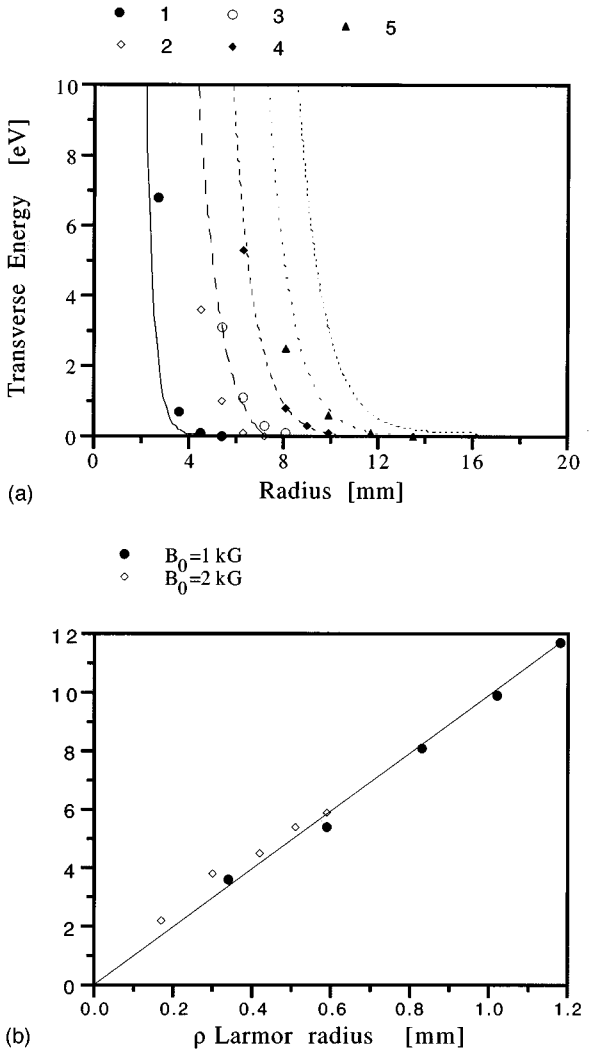

FIG. 4. Results of measurements and calculations for the geometry of a low-perveance gun (3.8 μP). (a) Transverse energy as a function of the beam radius for different anode potentials (1) 0.1, (2) 0.3, (3) 0.6, (4) 0.9, and (5) 1.2 kV. The lines show the results of simulation for the corresponding states. B_0=1 kG, $U_t=U_a$, U_{refl}=0. (b) Disturbance region diameter as a function of Larmor radius $R_0-(2eU_a/m)^{1/2}\cdot(mc/eB_0)$, where e and m are the charge and the mass of the electron and c is the light speed.

from the cathode exceeds the value of P_0, a jump in D_d value is practically observed. The curve in Fig. 5 illustrates the need for a precise current tuning to obtain a small disturbance region. Note that the reflector potential is optimized in all measurements of the curve in Fig. 5.

An important addition to this result are the measurements concerning the disturbance region for guns with different perveance values P_g in conditions with a high saturation current. The mark 1 in Fig. 5 indicates the value of D_d for a gun with $P_g<P_0$ (P_g=3 μP, $P_0\sim$12 μP); mark 3 is for a case $P_g\sim P_0$, and mark 4 is plotted for $P_g>P_0$.

Figure 6 shows corresponding curves for the minimum value of disturbance region diameter as a function of the beam current for these guns.

Actually, the results of simulations and experiments are consistent only for cases $P_g<P_0$ (as shown from the comparisons provided in Fig. 4). The case when $P_g\geqslant P_0$ (figures following Fig. 4) and the saturation current is more than I_0 is

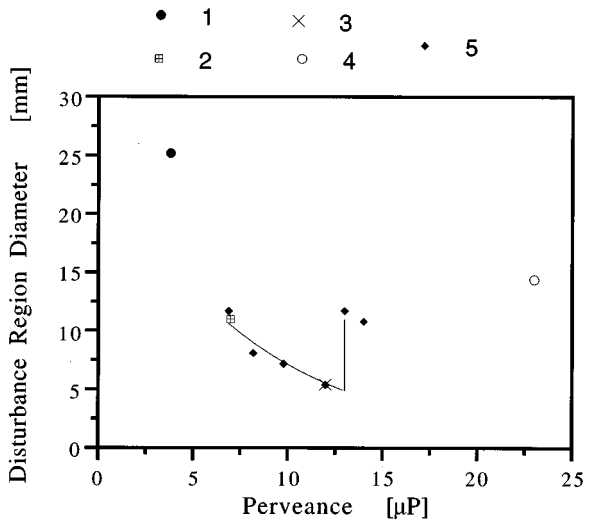

FIG. 5. Disturbance region as a function of the gun perveance. Points labeled by 1–4 show values of D_d for a space-charge limit current condition of a region near the cathode and different gun geometries. The values of P_g are equal for different signs, i.e., 1–3.8, 2–7, 3–12, and 4–23 μP. Points labeled by 5 indicate results for a fixed geometry (P_g=14 μP) and beam perveance changed by cathode saturation current (by heater current). For all data B_0=1 kG, $I\sim$100 mA, potentials are optimized.

rather complicated, and computer simulations can provide only qualitative information. Here, a region with zero potential is formed near the axis due to the influence of the space charge. The inner part of the beam is reflected from this region; the beam becomes tubelike and its current is less than $P_g\cdot U_a^{3/2}$. Similar phenomenon is known for the case of a solid cylindrical beam emitted into a tube. If the beam perveance is higher than the limit perveance of the tube, it also becomes tubelike.[10] In the experiment, we can observe this beam shape as a light irradiated by the electrons hitting the analyzer's collector surface. In the state with reflected electrons and the tube-shaped beam, the electron temperature is always higher than in conditions without reflection, and the

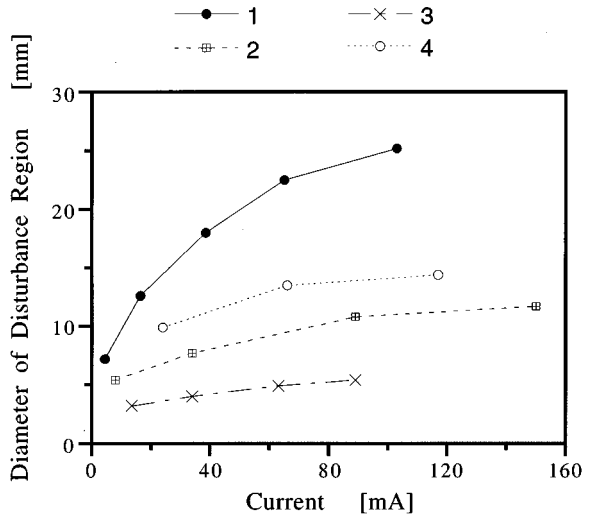

FIG. 6. Disturbance region diameter as a function of the beam current for guns with a different value of P_g:1–3.8, 2–7, 3–12, and 4–23 μP. B_0=1 kG.

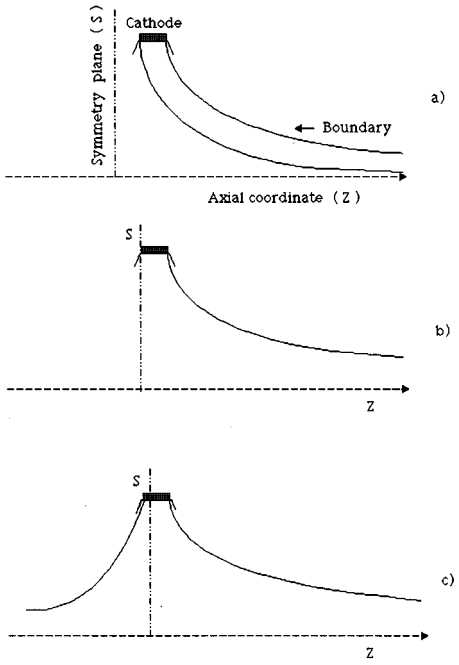

FIG. 7. Illustration of an opportunity to generate a hollow beam by shifting the magnetic field symmetry plane (S).

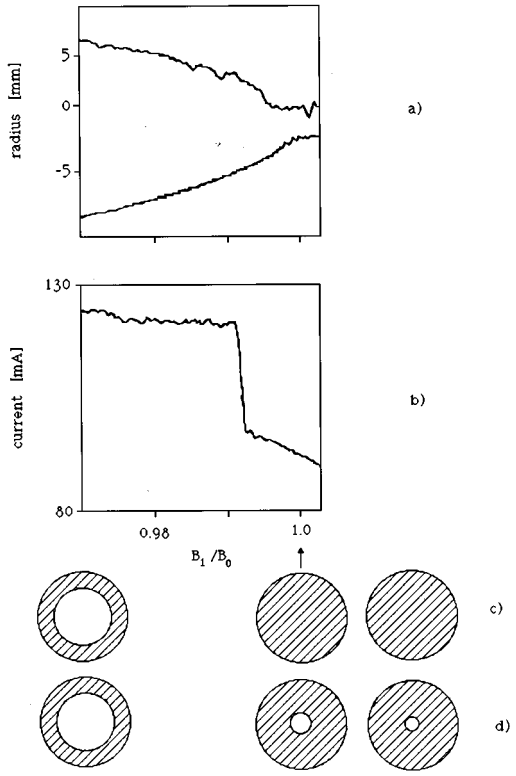

FIG. 8. Beam characteristics as a function of a ratio of the two oppositely magnetic field generated by the oppositely polarized solenoids (see Fig. 7). (a) Coordinates of hole boundaries. (b) Beam current. (c) and (d) Illustrations for pictures of magnetic fluxes from the cathode (c), and beam images at the analyzer collector surface (d). U_a=400 V, U_{ube}=2.3 kV, U_{refl}=−80 V, B_0=1 kG. The perveance is P_g=15 μP.

energy spread in the laboratory frame increases 3–5 times (the higher the beam current, the larger the increasing factor). This state is therefore of no interest for electron cooling purposes. However, the conditions with a high perveance P_g can be used if the hole in the beam is created by shifting the magnetic field symmetry plane (a plane marked as S in Fig. 7) from the cathode's edge [Fig. 7(a)]. Such a displacement δZ occurs, when the ratio B_1/B_0 of the colliding fields that create the cusp changes. As calculation shows, the value of δZ is proportional with a fair degree of accuracy to the difference between these fields:

$$\delta Z = L\left(1-\frac{B_1}{B_0}\right), \tag{8}$$

where L=23 mm.

Equating the magnetic fluxes inside the inner trajectory on the cathode and in the drift region:

$$B_c \cdot \delta Z \cdot 2 \cdot \pi R_c = B_0 \cdot \pi \cdot R_h^2 \tag{9}$$

the hole radius R_h can be established:

$$R_h = \sqrt{\frac{2B_c}{B_0} R_c dZ} = \sqrt{\frac{2B_c}{B_0} R_c L\left(1-\frac{B_1}{B_0}\right)}, \tag{10}$$

where R_c is the cathode radius, and B_c and B_0 are the magnetic field strength on the cathode surface and in the drift region, respectively.

The shift in the symmetry plane offers additional opportunities to investigate the states with the minimum possible size of the disturbance region. Figure 8 shows the hole radius and the beam current as functions of a ratio B_1/B_0.

The hole radius decreases with B_1/B_0, in agreement with Eq. (10), when this ratio is small enough. In such conditions, the beam is formed in the shape of narrow ring which can go through region II without reflection. When $B_1=B_0$, the magnetic field symmetry plane coincides with the cathode edge. In this case, the magnetic flux passing through the cathode surface changes into a solid cylinder [Figs. 7(b) and 8(c)]. Since $P_g>P_0$, a state with a current I_b is established, in which the beam becomes hollow and

$$I_0<I_b<P_g \cdot U_a^{3/2}. \tag{11}$$

The diameter of the disturbance region just before the current jump in Fig. 8(b) is considered as a value of D_d for the case $P_0<P_g$ (curve 3 in Fig. 6). If B_1 increases more than B_0, the symmetry plane moves on the cathode surface. Only electrons emitted to the right of the symmetry plane [Fig. 7(c)] can go out of the gun. The beam current is therefore proportional to the share of the cathode surface to the right of the plane and drops approximately linearly with B_1/B_0. The experimental curve (Fig. 8) is fairly consistent with this simple model and an estimation using (10). In this state, the electron temperature is also high.

One of the characteristic features of guns with $P_0<P_g$ is a hysteresis of the current (Fig. 9). This means that there is an interval of parameters where both states (with and without reflected electrons) are stable. This phenomenon is typical of space charge systems.[6] We found hysteresis for all tested guns with $P_g>P_0$, and the width of the hysteresis loop increases with the difference between P_g and P_0. The case of $P_g>P_0$ requires a more detailed investigation but is beyond the scope of this article.

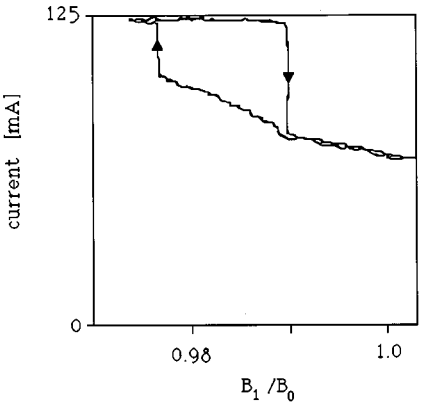

FIG. 9. Hysteresis in beam current as a function of B_1/B_0 ratio. B_0=1 kG, U_a=0.3 kV, U_{refl}=0, U_t=1.2 kV.

IV. DISCUSSION

In setting up the hollow cathode gun, our purpose was to fulfill requirements emerging from the ideal solution as much as possible. In the real gun, it is impossible to form electric fields completely coinciding with the ideal ones everywhere inside the electron beam. However, in the strong magnetic field, beam shape transformation occurs strictly along the magnetic field lines for the main part of the beam, where there is consequently no need to form precisely ideal electric fields. An exception is a region near the axis, where the magnetic field is weak and electron motion is disturbed. In our opinion, the only way to decrease a disturbance region's size is to create the potential and electric field distributions near the zero magnetic field point as close as possible to the ones in the ideal solution, i.e., a virtual cathode without reflected electrons. Experiments show that, in the real gun, it is possible to approach the state of the virtual cathode and generate the beam with a disturbance region size much smaller than the beam diameter.

ACKNOWLEDGMENTS

The authors acknowledge the useful discussion with N. S. Dikansky and V. V. Parkhomchuk, the participation of V. B. Chernishov in manufacturing the cathode, and of V. M. Barbashin in designing the electron gun, the assistance of T. N. Andreyeva for the calculations, and of V. M. Rybkin in mounting the prototype. This work was supported by Grant No. NQG300 from the ''International Science Foundation'' and by Contract No. ERB 4050PL 94-1414 from the ''European Community.''

[1] G. I. Budker, *Proceedings of International Symposium on Electron and Positron Storage Rings Saclay, 1966*, edited by H. Zyngier and E. Cremienx-Alcan (PUF, Paris, 1967), p. II-1-1.
[2] A. N. Sharapa and A. V. Shemyakin, Nucl. Instrum. Methods Phys. Res. A **336**, 6 (1993).
[3] G. Bisoffi *et al.*, LNL-INFN Internal Report 80/94 (unpublished).
[4] V. M. Barbashin *et al.*, Nucl. Instrum. Methods Phys. Res. A **366**, 215 (1995).
[5] A. N. Sharapa and A. V. Shemyakin, Nucl. Instrum. Methods Phys. Res. A **289**, 14 (1990).
[6] H. F. Ivi, Adv. Electron. Electron Phys. **6**, 137 (1954).
[7] A. N. Sharapa, Nucl. Instrum. Methods Phys. Res. A **329**, 551 (1993).
[8] D. M. Myakishev *et al.*, Int. J. Mod. Phys. A **2B**, 915 (1993).
[9] V. I. Kudelainen *et al.*, JETP **56**, 1191 (1982); A. V. Alexandrov *et al.*, Meas. Sci. Technol. **4**, 764 (1993).
[10] D. D. Ryutov, J. Technol. Phys. **47**, 709 (1977) (in Russian).